Test Structures for Studying Coplanar Reverse-Electrowetting for Vibration Sensing and Energy Harvesting

Anotidaishe Moyo[1], Muhammad Wakil Shahzad[1], Jonathan G. Terry[2], Stewart Smith[2],

Yoshio Mita[3], Yifan Li[1]

[1]Department of Mechanical and Construction Engineering, Faculty of Engineering and Environment,

Northumbria University, Newcastle upon Tyne, NE1 8ST, UK

[2]School of Engineering, Institute for Integrated Micro and Nano Systems,

The University of Edinburgh, Edinburgh, EH9 3FF, UK

[2]Department of Electrical Engineering and Information Systems, The University of Tokyo, Tokyo, Japan

Abstract *Reverse electrowetting on dielectric (REWOD) has emerged to be a promising energy harvesting technology from low frequency vibrations. This study aims to use test structures to characterize a unique form of REWOD using a coplanar electrode configuration. This configuration allows for better versatility in system integration, device packaging and applications.*

Keywords *Reverse-Electrowetting on Dielectric, Electric Double layer, Energy Harvesting*

I. Introduction

Reverse Electrowetting on Dielectric (REWOD) has emerged as a promising energy harvesting technology that can harness kinetic energy from liquid droplet deformation driven by mechanical movements (e.g. vibration, falling raindrops, etc.) As its name suggests, REWOD is a reversal of the electrowetting on dielectric phenomenon where liquid droplets deform and move around driven by electrical energy [1]. In REWOD, when the droplet shape oscillates, the liquid-solid contact area change results in a significant capacitance change, causing the displacement of electrical charges in the circuit model shown in Figure 1a. The generated energy can be measured through a connected load (e.g. a RIGOL DS1054Z scope set to 1 MΩ). Until now, most studies have employed a "two-plate" REWOD configuration (Figure 1b) where both top and bottom structures contain conductive electrodes, a counter electrode (CE) on the top, and a dielectric-layer-coated energy-harvesting electrode (EHE) at the bottom, with a bias voltage applied across them [2-4]. Both plates also have thin amorphous fluoropolymer (aFP) hydrophobic coatings to maximize the starting height (g_{max}) of a droplet and minimize the starting droplet-surface contact area A_{min}, which is to enable a large change of area ΔA during the oscillation.

In recent years, some coplanar "one-plate" REWOD configurations (Figure 1c) have emerged, which do not have the restricted conditions that result from the presence of the top plate [5, 6]. For example, this configuration has huge potential in raindrop energy harvesting [5], as well as flexible force/motion sensing/energy harvesting [6]. However, no published work can be found which focuses on coplanar REWOD electrode design and fabrication considerations. This leaves a noticeable knowledge gap in the optimization of energy conversion efficiency through structure design improvements.

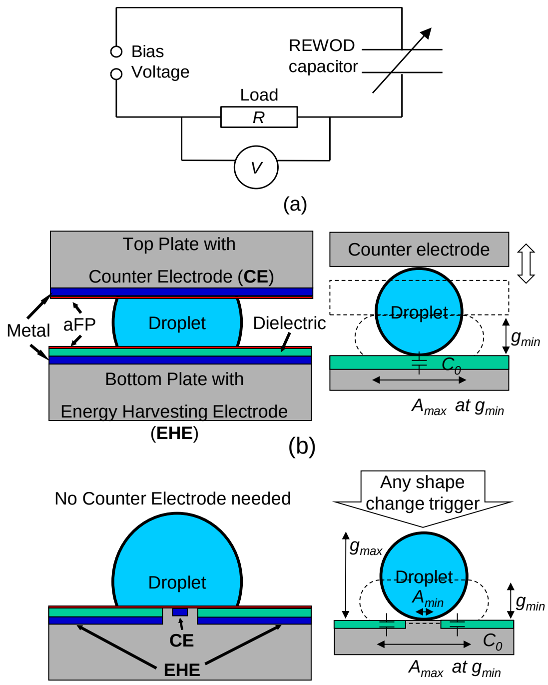

Figure 1. (a) Schematic of an REWOD energy harvesting circuitry; (b) Side view of common "two-plates" REWOD working mechanism, where counter electrode (CE) and energy harvesting electrode (EHE) are located on two parallel plates; (c) Side view of coplanar REWOD configuration, where CE and EHE both situate on the bottom plate, leaving design flexibility on top structures.

II. TEST STRUCTURE DESIGN AND METHODOLOGY

This paper proposes REWOD co-planar test structures (Figure 2) along with a characterisation mechanism based on a similar concept used to evaluate co-planar EWOD reported in [1]. The aim is to study the effect of electrode design on the efficiency of energy conversion achievable.

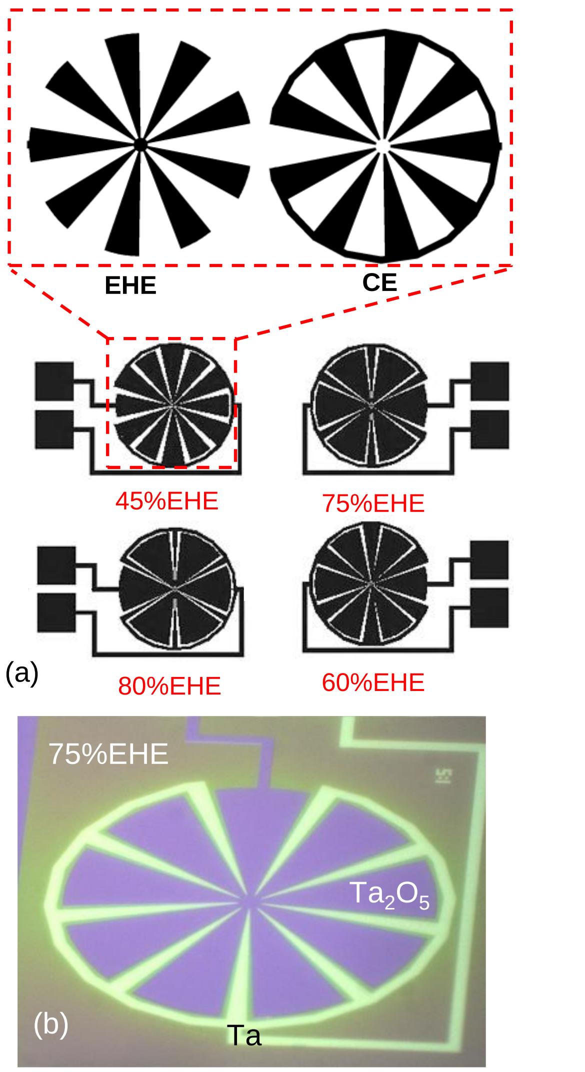

Figure 2. (a) Top view of test structure designs which maintain EHE:total area ratio during droplet spreading; (b) A close-up image of the fabricated test structure (EHE:total area ratio 75%), where the EHE has 95nm Ta_2O_5 dielectric coating.

To ensure the solid-liquid contact area over the EHE remains at a constant ratio to the overall contact area during the spreading/deformation of a centred droplet, these test structures were designed to have interdigitated EHE and CE electrodes in symmetric "flower petal" shapes, as shown in Figure 2a. Figure 2a also shows the designed test structures with different EHE and CE area ratios. For the 45% EHE structure, the CE had the same area ratio to EHE (45%), while the gap area between the two occupied 10% of the total area. For the 60%, 75% and 80% EHE structure, the gap area between CE and EHE still occupied 10% of the total area, while the remaining 90% area was divided in CE:EHE ratios of 1:2, 1:5 and 1:8 respectively. The gap area ratios could also vary in test structure designs to give a potential range of the EHE:total area ratios of between 20% to 80%.

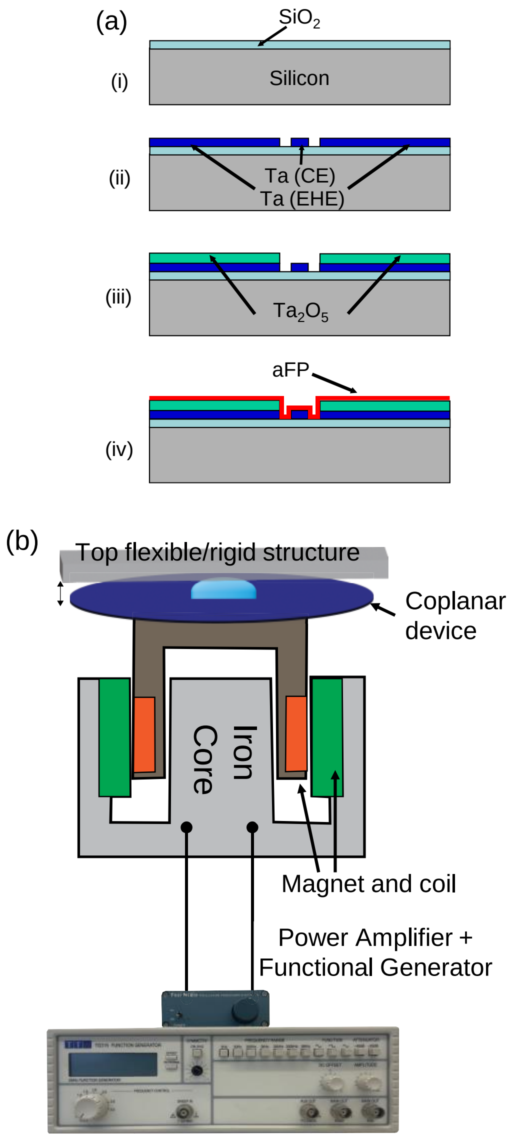

Figure 3. (a) Fabrication process of the coplanar test-structure devices in cross-sectional view; (b) Schematic of the experimental set-up showing the characterization system with voice coil actuator driven vibration causing the droplet shape oscillation as the mechanical input. The coplanar test structures are connected to an oscilloscope (1 MΩ input impedance) to characterize the output electrical energy.

Figure 3a shows the fabrication process of the test structures. A 500 nm SiO_2 insulation layer was thermally grown on a silicon substrate. This was followed by the sputtering deposition and photolithography patterning of a 500 nm of Tantalum layer that forms the EHE and CE electrodes. The EHE Tantalum electrodes were then selectively anodized in a similar way reported in [1] to create a high-κ thin Ta_2O_5 layer (95 nm) with dielectric constant of 18. At the end of the process, the entire coplanar device is coated with 35nm of amorphous fluoropolymer (aFP) hydrophobic layer.

To characterise the energy conversion efficiency, the experimental setup shown in Figure 3b was used. The mechanical vibration input is provided by a voice coil actuator driven by a functional generator (TTi TG315) and power amplifier (Fosi Audio TPA3116). The input vibration frequencies were set in the range of 0.75 to 20 Hz.

Although a top counter electrode (CE) is not required in this coplanar configuration, a vibrating top plate (without a metal electrode) is used to help control the droplet deformation/spreading process as shown in Figures 1c and 3b. An acrylic plate coated with aFP hydrophobic coating is used together with a spacer to control the minimum droplet height g_{min} = 0.7 mm (Figure 1c). Two different DI (de-ionized) water droplet sizes were used: 10 and 20 µL. This translates into a maximum droplet spreading area (Fig. 1c) of A_{max} =14.29 and 28.57 mm^2 respectively.

In a two-plate configuration, the energy generated in one oscillation period is governed by equation 1:

$$E = \frac{5}{4} V^2 C_0 \left[1 - \tanh\left(\frac{1}{2}\left(1 - \ln(\omega R C_0)\right)\right)\right] \quad \text{(EQ1)}$$

where V is the bias voltage, $\omega = 2\pi T^{-1}$ is the capacitance oscillation frequency, T is the characteristic period of one wetting-dewetting cycle, R is the load (i.e. input impedance of the oscilloscope), and C_0 is the EHE capacitance when a droplet is at the maximum deformation (representing a maximum value of the variable capacitor in Figure 1a). For 10 and 20 µL droplets, C_0 = 5.55 and 11.1 nF respectively, at A_{max} due to the 95 nm Ta_2O_5 dielectrics and 35 nm aFP hydrophobic coating combination.

For the co-planar test structure, the model needs to be modified. The effect of the coplanar electrode area ratio on the capacitance in the system can be estimated to be:

$$C_{cop} = \frac{A_{EHE}}{A_{total}} C_0 \quad \text{(EQ2)}$$

where A_{EHE}/A_{total} is the EHE:total area ratio. Other design considerations can also be investigated with the test structures, such as whether the CE should also be covered by a dielectric layer – a key factor in optimising the energy harvesting efficiency. Figure 2b shows a fabricated 75% EHE test structure, where a 95 nm thick anodic Ta_2O_5 dielectric layer covers the EHE, while the tantalum CE electrode is only covered by a thin aFP hydrophobic coating.

III. Results and Conclusion

For each experiment, a single droplet on a single test structure was used for the energy harvesting characterisation. Similar to work in [2], the single droplet "unit" instantaneous output electrical power could be calculated from the output voltage measured by the RIGOL DS1054Z oscilloscope with 1MΩ impedance (the load in Figure 1a). The voice coil actuator was initially operated at 1 Hz, however the measured characteristic period of one wetting-dewetting cycle T was estimated to be around 1.5 milliseconds (ms) from the displayed oscilloscope waveform due to the actuator being driven more as if in pulse mode.

Therefore, based on equation 1, the calculated unit energy values generated in one wetting-dewetting period with droplet sizes of 10 µL and 20 µL and EHE:total area ratios of 60% and 80% can be calualated as shown in Table 1 below. Using A_{max} as the unit area, energy generation power density was calculated as $P = E/A_{max}$:

TABLE I. CALCULATED ENERGY AND POWER DENSITY PER CYCLE

Drop vol. (µL)	*EHE ratio*	*Energy E (µJ)*	*Power density P (W/m²)*
10	60%	0.575	30.18
10	80%	0.796	41.78
20	60%	1.241	32.58
20	80%	1.689	44.33

Figure 4 shows the instantaneous power generation per unit area results derived from the peak voltage readings from the oscilloscope ($P_{inst} = V^2/R \times A_{max}$), similar to other work such as in [2]. All the measured values are divided into four quartiles and presented. The median results are labelled and placed in the box indicating second and third quartiles.

Comparing Table 1 and Figure 4, the experimental power density results are in the same order of magnitude as the theoretical calculations, and found to be close to other published work such as [2]. For 20 µL droplet tests, 80% EHE provided proportionally higher energy density as expected. However, it is interesting to see that, for the 10 µL droplet, the effects of changing the EHE:total area ratio are not as clear. They have very similar median values, and contrary to the calculation, both the minimum and maximum instantaneous powers observed are higher for the 60% EHE ratio. Experimentally, more difficulties were experienced attempting to centre the smaller droplets during the wetting and de-wetting processes, which may explain these results. While the 10 µL droplet resulting in higher power generation density disagrees with the calculation in Table 1, a similar effect has been observed by others, such as [2]. One possible reason could be the smaller droplet having a different wetting-dewetting cycle period T, but this needs further investigation.

Figure 4. Showing the measured instantaneous electric power for (left) 20µL droplet at 1Hz modulation for the 80% and 60% EHE ratios; and (right) 10µL

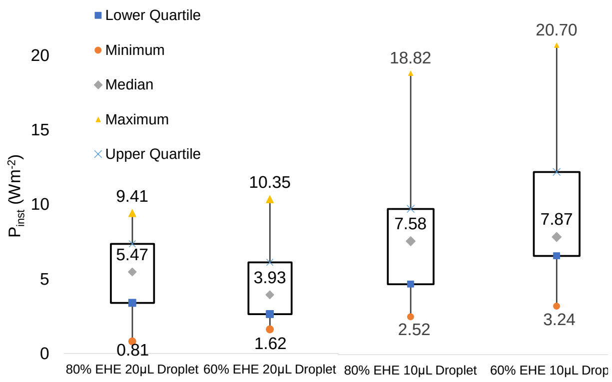

droplet at 1Hz modulation for the 80% and 60% EHE ratios. The boxed regions show data (frequency) in second and third quartiles.

In conclusion, we have shown that the REWOD test structures can be used to inform the design of energy harvesting devices with optimised energy conversion efficiency in a coplanar configuration, something which has not been studied systematically to the authors knowledge. A coplanar theoretical model has been established and modified from a conventional two-plate version, with calculated power generation density (averaged over a single wetting-dewetting cycle) close to the measured instantaneous values.

This development has revealed an interesting research direction for coplanar REWOD system design optimisation. Future work will study the relationship between droplet size and EHE:total area ratio, while considering other factors such as droplet height change and wetting-dewetting cycle time in coplanar configurations.

ACKNOWLEDGMENT

We acknowledge Dr Camelia Dunare and Mr Stewart Ramsay, who fabricated the test structures in the cleanroom facilities of the Scottish Microelectronics Centre, at the University of Edinburgh. The authors would like to thank MEMSstar Ltd, who provided access to their aFP hydrophobic coating AURIX^{TM} system. The authors would also like to thank the financial support from EPSRC ReNU Centre for Doctoral Training (CDT) fund (EP/S023836/1).

REFERENCES

[1] Li, Y., et al., *Test Structure for Characterizing Low Voltage Coplanar EWOD System.* Semiconductor Manufacturing, IEEE Transactions on, 2009. **22**: p. 88-95.

[2] Krupenkin, T. and J. Taylor, Reverse electrowetting as a new approach to high-power energy harvesting. Nature communications, 2011. **2**: p. 448.

[3] Liu, K., et al., *Self-Powered Multimodal Temperature and Force Sensor Based-On a Liquid Droplet.* Angewandte Chemie International Edition, 2016. **55**(51): p. 15864-15868.

[4] Adhikari, P.R., et al., Reverse Electrowetting-on-Dielectric Energy Harvesting Using 3-D Printed Flexible Electrodes for Self-Powered Wearable Sensors. IEEE Sensors Letters, 2022. **6**(5): p. 1-4.

[5] Xu, W., et al., A droplet-based electricity generator with high instantaneous power density. Nature, 2020. **578**(7795): p. 392-396

[6] A. Moyo, M. W. Shahzad, J. Terry, Y. Mita and Y. Li, "A facile coplanar reverse electrowetting-on-dielectric configuration for more flexible and integratable force/motion sensing applications," *2022 IEEE Sensors*, 2022, pp. 1-5

[7] Helseth, L.E. and X.D. Guo, Contact Electrification and Energy Harvesting Using Periodically Contacted and Squeezed Water Droplets. Langmuir, 2015. **31**(10): p. 3269-3276.

[8] Lin, S., X. Chen, and Z.L. Wang, *Contact Electrification at the Liquid–Solid Interface.* Chemical Reviews, 2021.

[9] Moon, J.K., et al., *Electrical power generation by mechanically modulating electrical double layers.* Nature Communications, 2013. **4**(1): p. 1487.

[10] Adhikari, P.R., R.C. Reid, and I. Mahbub, *High power density and bias-free reverse electrowetting energy harvesting using surface area enhanced porous electrodes.* Journal of Power Sources, 2022. **517**: p. 230726.

[11] Tasneem, N.T., et al., *Design of a Reverse-Electrowetting Transducer Based Wireless Self-Powered Motion Sensor.* 2020 IEEE International Symposium on Circuits and Systems (ISCAS), 2020: p. 1-5.

[12] Yang, H., et al., High-performance reverse electrowetting energy harvesting using atomic-layer-deposited dielectric film. Nano Energy, 2017. **31**: p. 450-455.